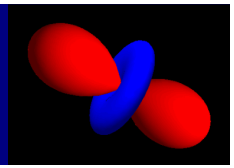

Low-dimensional magnetism in DFT

G. Radtke
IMPMC UMR 7590 CNRS, Université Pierre et Marie Curie
(previously @ IM2NP UMR 7334 CNRS, Aix-Marseille Université)

A. Saúl
CiNAM UMR 7325 CNRS, Aix-Marseille Université

G. Rousse, Y. Klein
IMPMC UMR 7590 CNRS, Université Pierre et Marie Curie

Materials modeling @ IMPMC

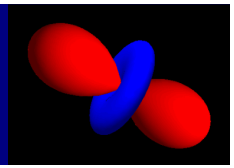

People working on modelisation in the lab :

Ch. Brouder (DR-CNRS sec. 3)
D. Cabaret (MdC-Paris 6)
M. Calandra (DR-CNRS)
M. Casula (CR-CNRS, sec. 3)
M. Lazzeri (CR-CNRS)
F. Mauri (DR-CNRS)
L. Paulatto (IR-CNRS)

M. Saitta (PR-Paris 6)
G. Ferlat (MdC-Paris 6)
M. Blanchard (CR1-CNRS sec. 18)
E. Balan (CR-IRD)
A. Juhin (CR1-CNRS sec. 5)
M.A. Arrio (CR1-CNRS sec. 5)
G. Radtke (CR-CNRS, sec. 15)

Quantum theory of materials with and beyond DFT

Prediction of materials properties based on ab initio meth

- 2D materials beyond graphene
- Molecular superconductivity
- Ab-initio theory of charge and heat transport in nanostructures
- Beyond DFT : Quantum Monte-Carlo

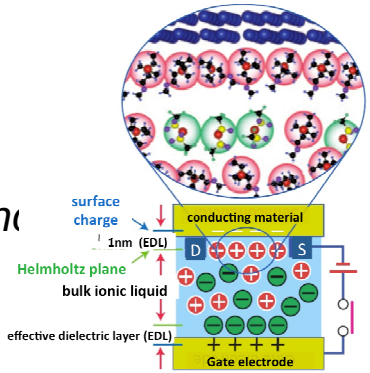

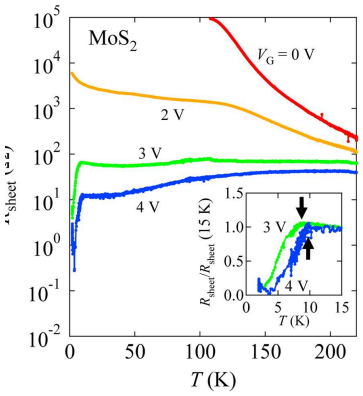

▲ **MoS_2 becomes metallic and superconducting once doped by K or Rb intercalation (Tc~10 K) or in a FET [Taniguchi et al., APL 101, 042603 (2012)]**

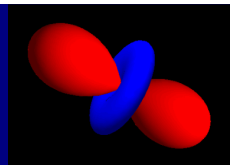

Disordered matter

Microscopic structure of liquids and glasses in high-pressure/high-temperature conditions with ab initio molecular dynamics

- structure of simple glasses and crystals (B_2O_3) [Nature Mat. 2012]
- polyamorphism under high temp./pressure in GeO_2 [PRB 2012]
- nucleation phenomena in glasses
- Ionic solvation in supercritical fluids [J. Chem. Phys. 2011]

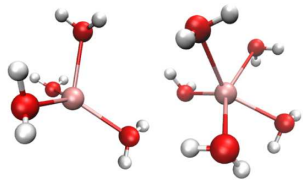

▲ **Ag^+ ions in supercritical water**

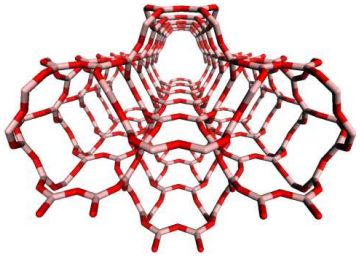

▲ **Prediction of a porous B_2O_3 polymorph.**

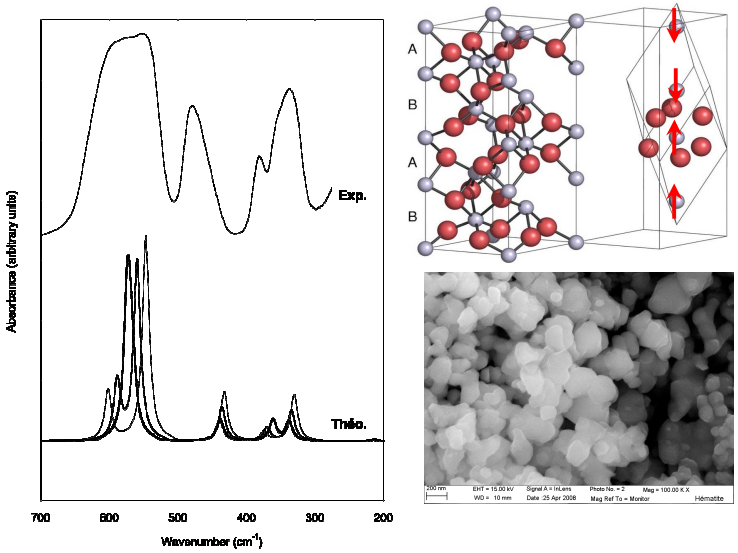

▲ **IR spectra in α-Fe_2O_3 and SEM image of the sample.**

Geomaterials

Vibrational and isotopic properties in minerals and molecules in DFT

- IR and Raman modeling in α-Fe_2O_3 [Am. Min. 2008
- Isotopic fractionation in cosmochemical processes [Earth Plan. Sci. Lett. 2012]

Materials modeling @ IMPMC

Condensed matter under extreme conditions

Theory of matter under extreme conditions
Ab initio calculation of phase diagrams, Raman spectra modeling, molecular dynamics

- Molecular dynamics of dissociation of Water under an electric field [PRL 2012]
- Pressure-induced polyamorphism in salty water [PRL 2011]
- Pressure-induced transformations of $AlPO_4$ [Nature Mat. 2007]

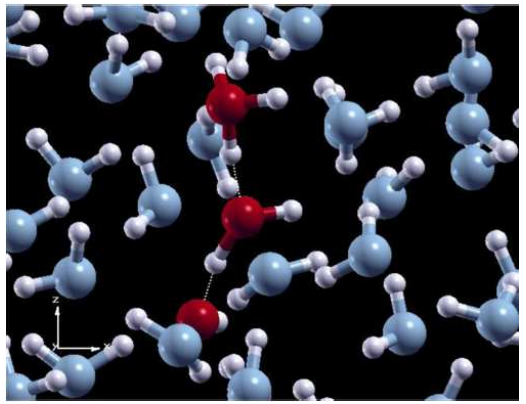

Snapshot of a typical dissociation-diffusion mechanism in water under an electric field

Core-level X-ray spectroscopies

XANES, XMCD, RIXS-MCD

- one-electron (Xspectra in Quantum Espresso)
- multi-electronic (ligand-field multiplets)

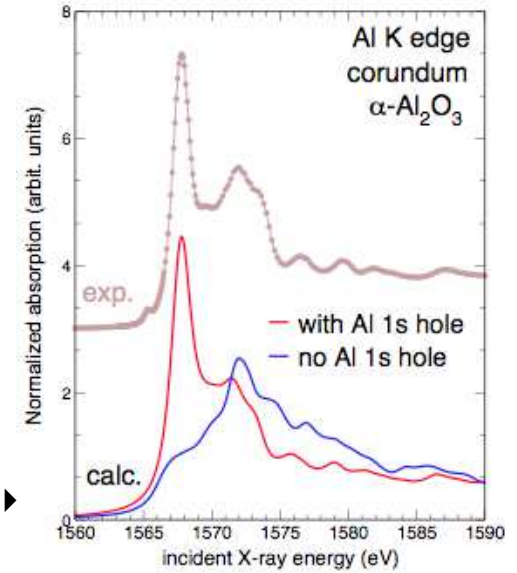

Core-hole effect on calculated Al-K edge in α-Al_2O_3.

Outline

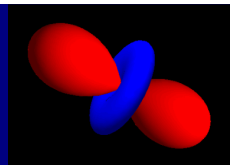

To interpret experiments, systems of localized moments are often modeled with Heisenberg Hamiltonians :

$$\hat{H} = \hat{H}_0 + \sum_{i>j} J_{ij} \hat{\mathbf{S}}_i \hat{\mathbf{S}}_j$$

The determination of the dominant couplings based on geometry is often difficult, sometimes misleading ...

Two surprising systems based on magnetic dimers revealed by DFT :

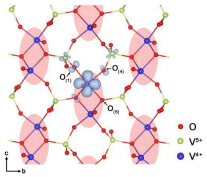

CsV_2O_5 :
where the magnetic dimers are NOT the structural dimers

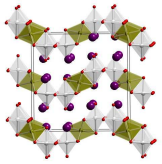

$Ba_4Ru_3O_{10}$:
where structural trimers behave as magnetic dimers

Localized magnetism in CsV_2O_5

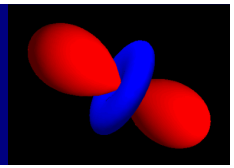

Monoclinic structure $P2_1/c$

Alternating layers of Cs and V_2O_5

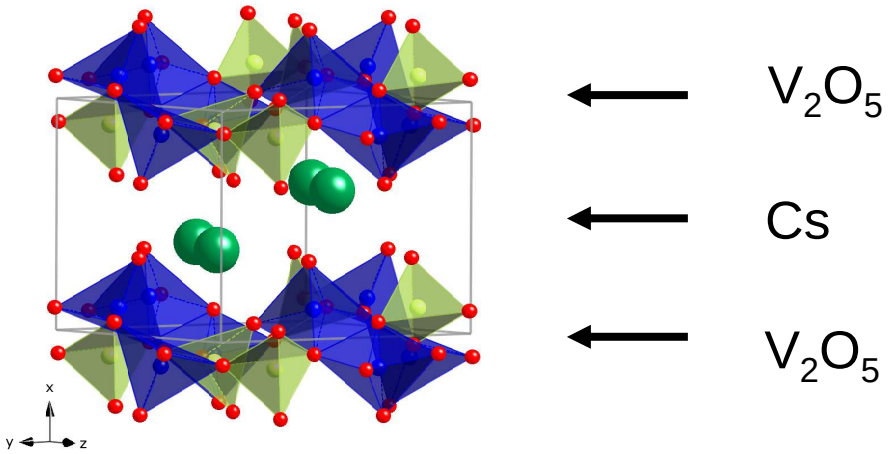

Structure of the layers

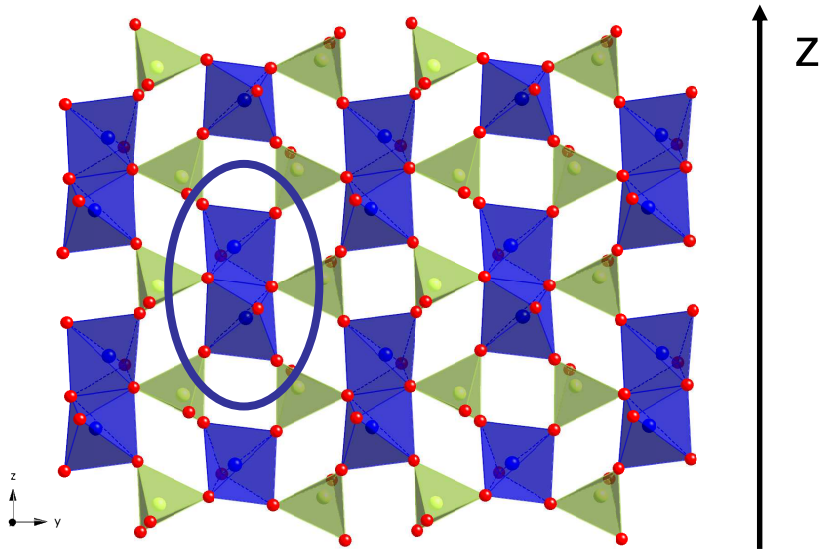

Two different V atoms in the layers

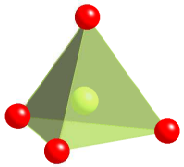

V^{5+} in tetrahedra

➡ non-magnetic ($3d^0$)

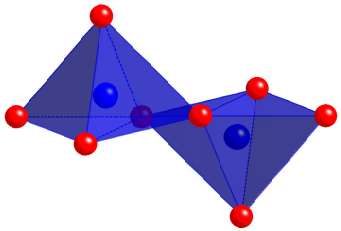

V^{4+} in distorted square pyramids sharing edges

➡ magnetic ($3d^1$)

Confirmation : the magnetic susceptibility

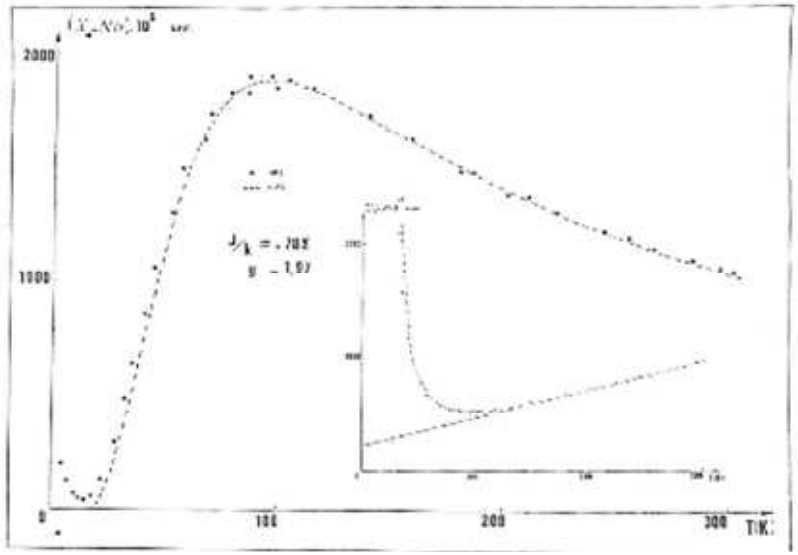

J. Mur and J. Darriet
C. R. Acad. Sc. Paris **300** (1985) 599

➡ Isolated dimers : J = 156 K

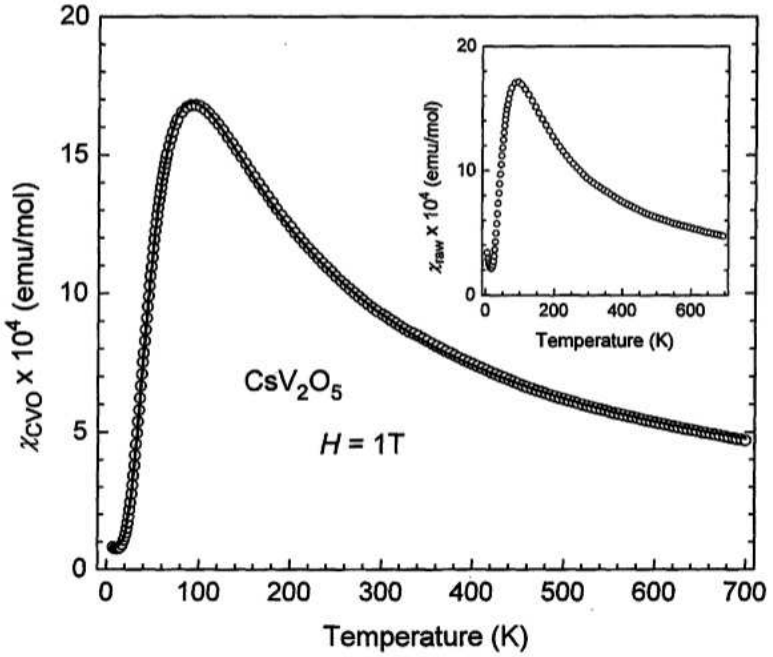

M. Isobe and Y. Ueda
J. Phys. Soc. Jap. **65** (1996) 3142

➡ Isolated dimers : J = 146 K

➡ Does DFT confirm this picture ?

Magnetic interactions in CsV_2O_5

$$\hat{H} = \hat{H}_0 + \sum_{i>j} J_{ij}\hat{\mathbf{S}}_i\hat{\mathbf{S}}_j$$

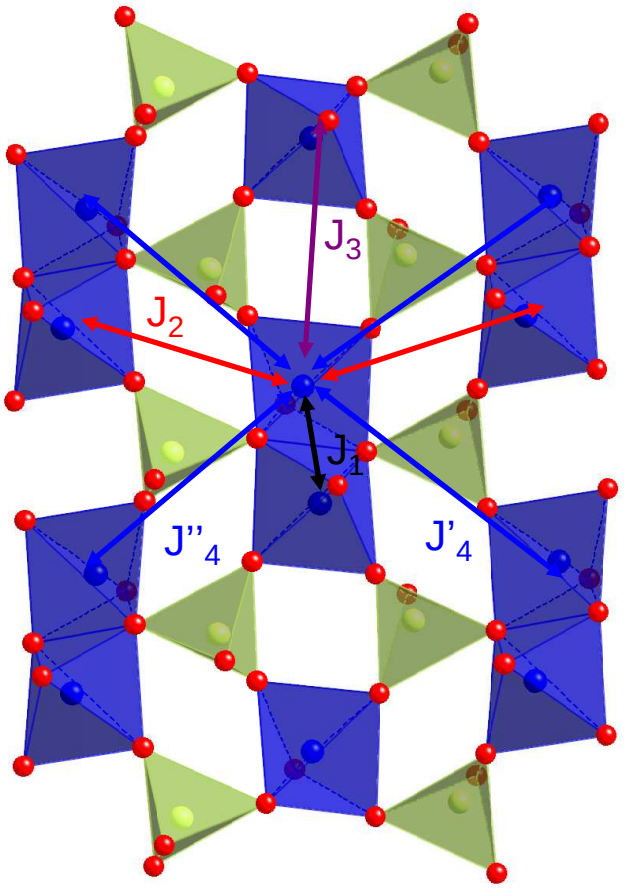

Magnetic couplings up to the fourth nearest neigbours :

J_1 (3.073 Å) intradimer
J_2 (5.386 Å) interchain
J_3 (5.503 Å) intrachain
J'_4 (5.950 Å) interchain
J''_4 (6.653 Å) interchain

Simplified J_4 interaction:

$J_4=(J'_4+J''_4)/2$

Mapping DFT energies : single dimer

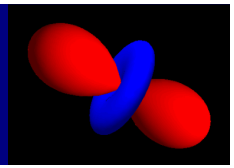

Estimation of J from DFT calculations?

A system formed by a single spin-1/2 dimer $\hat{H} = \hat{H}_0 + J\hat{\mathbf{S}}_1\hat{\mathbf{S}}_2$

Magnetic excitations written as a Heisenberg Hamiltonian

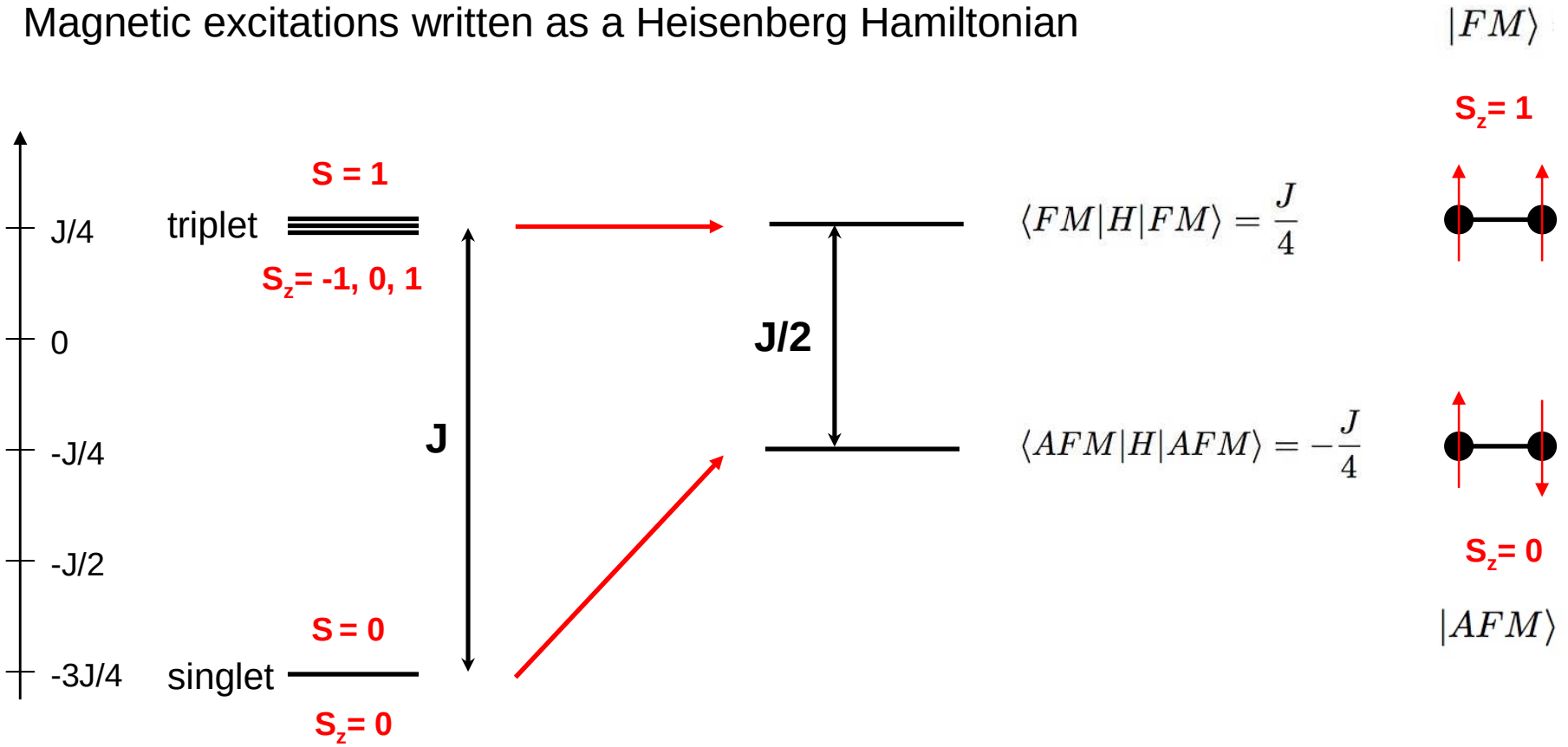

Spin contaminated nature of the AFM solution (not an eigenstate of S^2)

Calculation of the exchange interactions

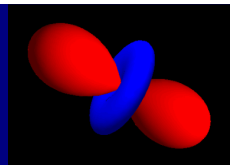

Heisenberg Hamiltonian for a general system

$$\hat{H} = \hat{H}_0 + \sum_{i>j} J_{ij} \hat{\mathbf{S}}_i \hat{\mathbf{S}}_j$$

Defining a DFT (collinear spin arrangement) state

$$|\alpha\rangle =$$

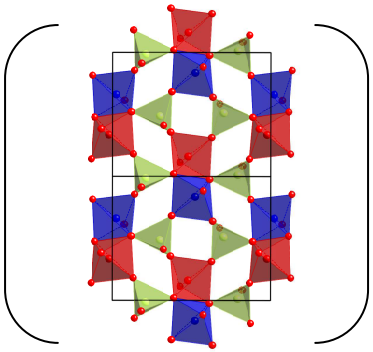

A Kohn-Sham state (determinant) with a given projection of the spin in atom *i*

$$\hat{S}_{iz}|\alpha\rangle = \pm\tfrac{1}{2}|\alpha\rangle$$

The mean value of the Hamiltonian (the DFT total energy) :

$$\epsilon_\alpha = \langle\alpha|\hat{H}|\alpha\rangle = \epsilon_0 + \sum_{i>j} \frac{J_{ij}}{4}\sigma_i\sigma_j \qquad \boldsymbol{\sigma_i = \pm 1}$$

can be written as an Ising Hamiltonian with the same J's

Spin configurations

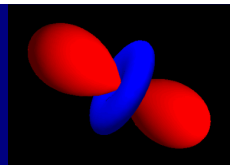

64-atom supercells (doubled along the chain direction z)

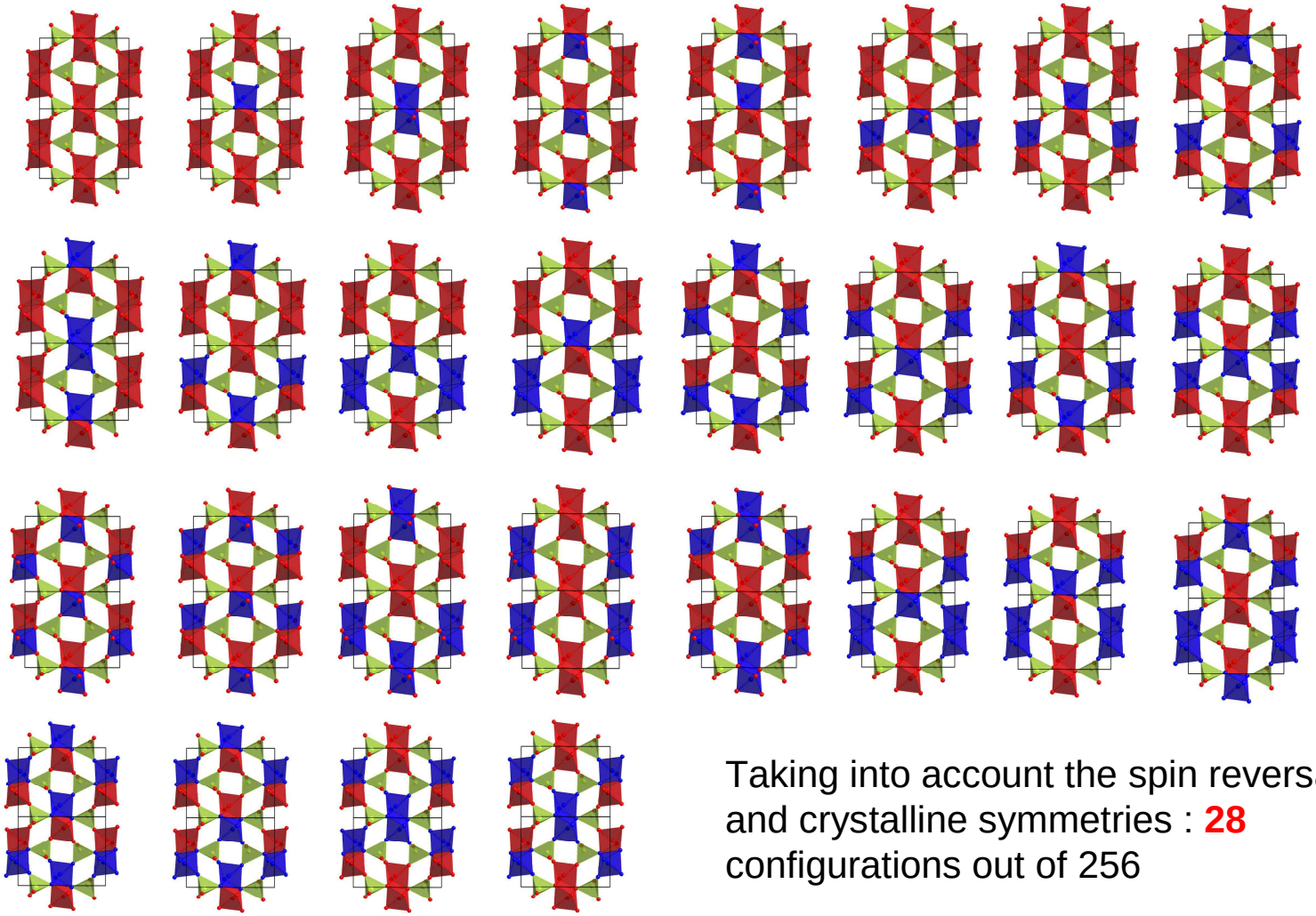

Taking into account the spin reversal and crystalline symmetries : **28** configurations out of 256

Mapping of DFT energies: fitting procedure

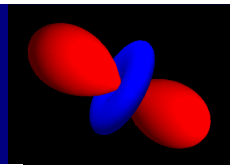

Optimisation of the Ising parameters

$$F = \sum_{\alpha=1}^{28} g_\alpha \left(\epsilon_\alpha - \epsilon_0 - \sum_{i=1}^{4} a_{i\alpha} J_i \right)^2$$

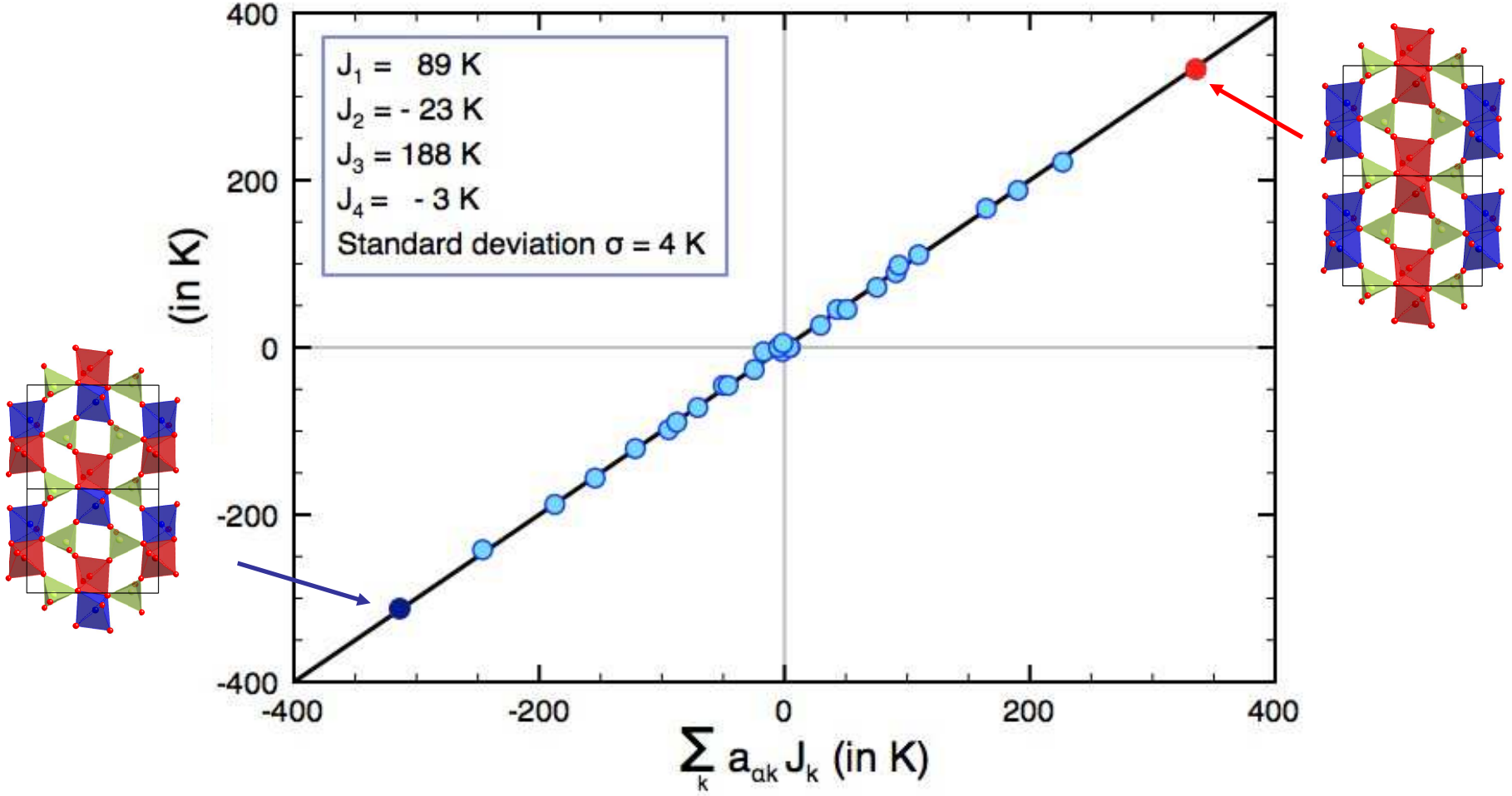

Numerical results

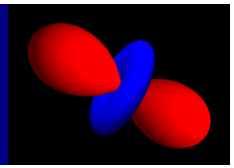

Ex. Int. (K)	J_1	J_2	J_3	J_4
PBE0	89	-23	188	-3
PBE	180	-54	378	-11

- Dominant AF interactions along the chain
- Third nearest- neighbor $J_3 > J_1$
- Weak and ferromagnetic inter-chain interaction
- A semi-local functional GGA increases the amplitudes by ~ 2 with respect to the exact exchange one

Proposed superexchange paths

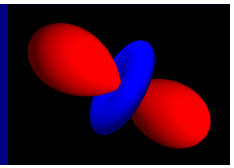

Motivated by the symmetry of the atomic orbitals

Close-to-orthogonal arrangement of the V^{4+}-*d* and O-*p* orbitals suggests a

Weak J_1

Non zero density of the V^{5+}-*d* orbital and allows a relatively

Large J_3

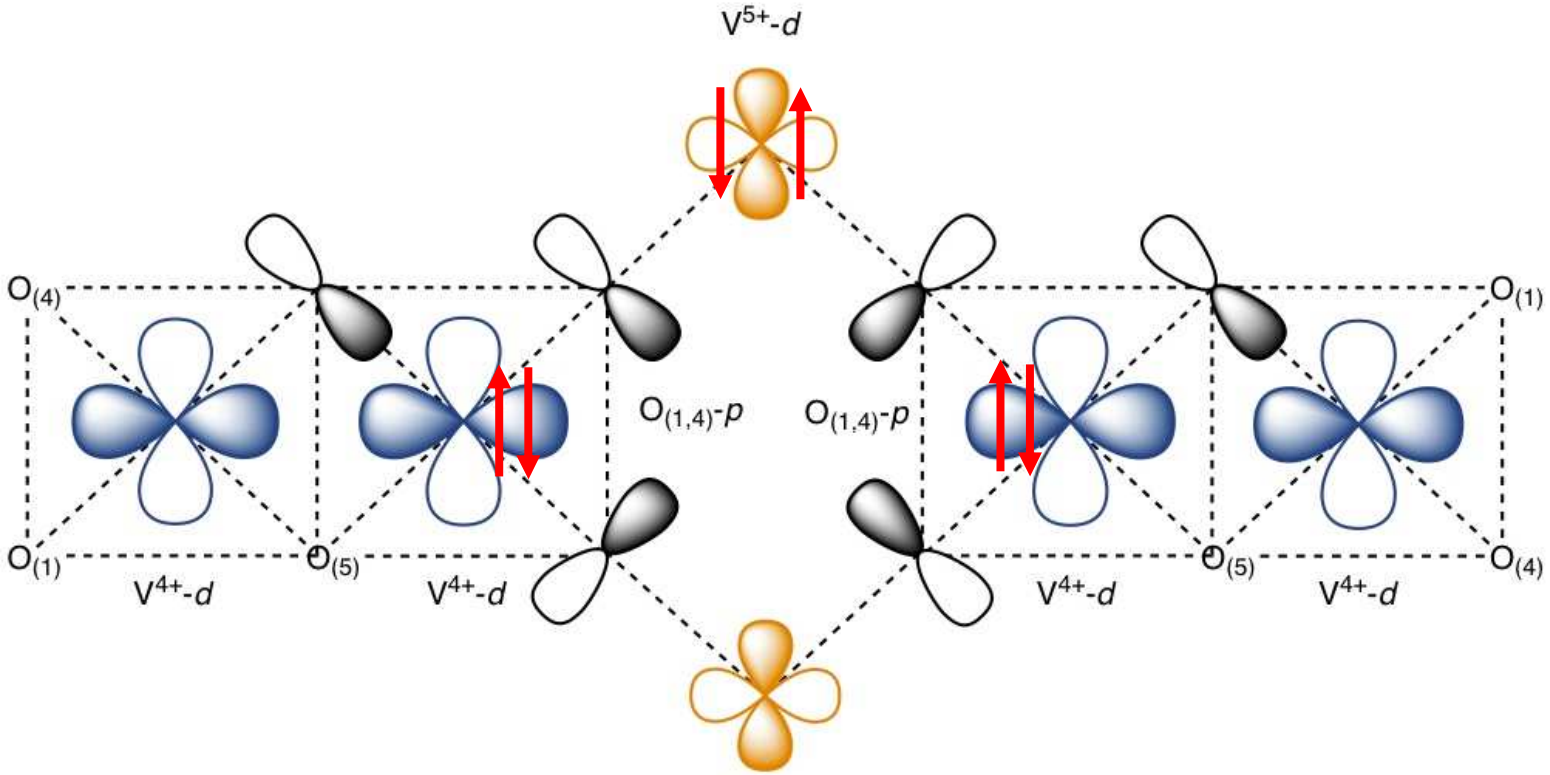

A “not so localized” system : $Ba_4Ru_3O_{10}$

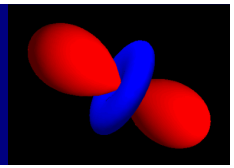

Orthorhombic structure *Cmca*
2D layers of Ru_3O_{12} trimers

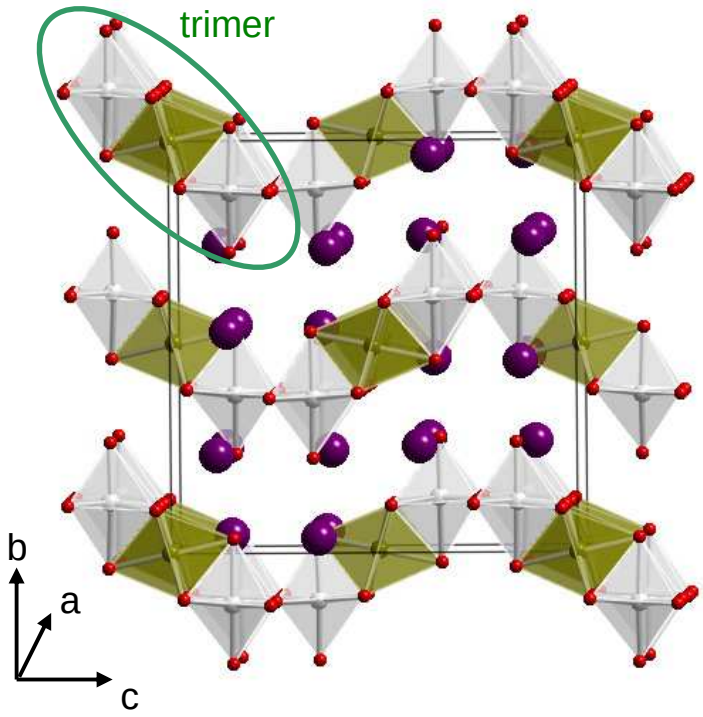

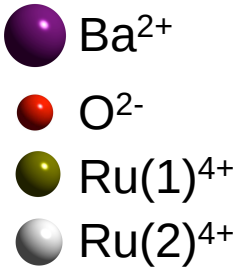

Structure of the layers

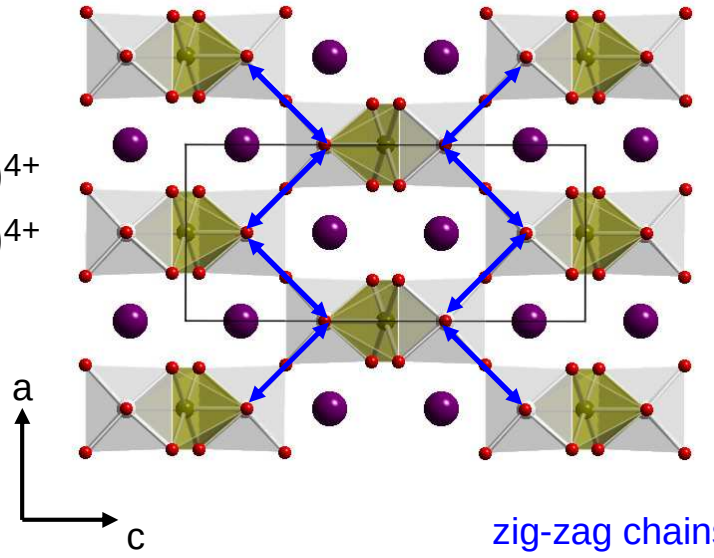

zig-zag chains along **a**

Face-shared Ru_3O_{12} trimers bring Ru ions very close (2.55Å)

➡ possibility of metal-metal bonding

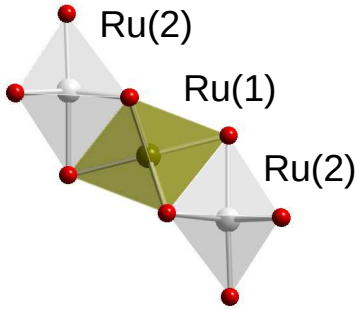

Experimental results

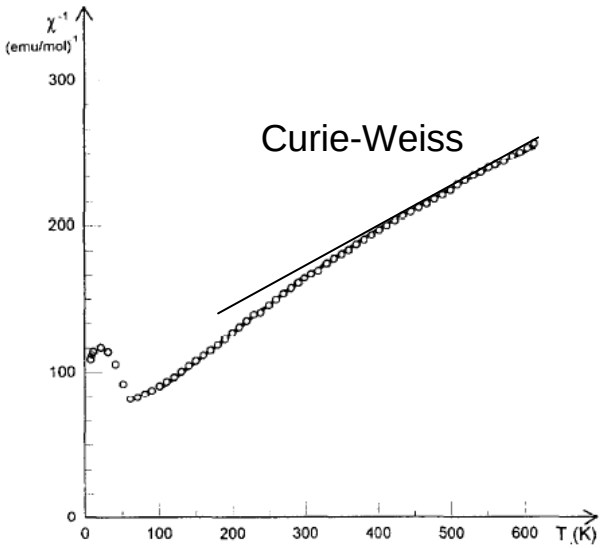

Fig. 6. Thermal variation of the reciprocal susceptibility of $Ba_5Ru_3O_{12}$ (circles, observed; full line, calculated).

C. Dussarat *et al.*
J. All. Comp. **233** (1996) 15

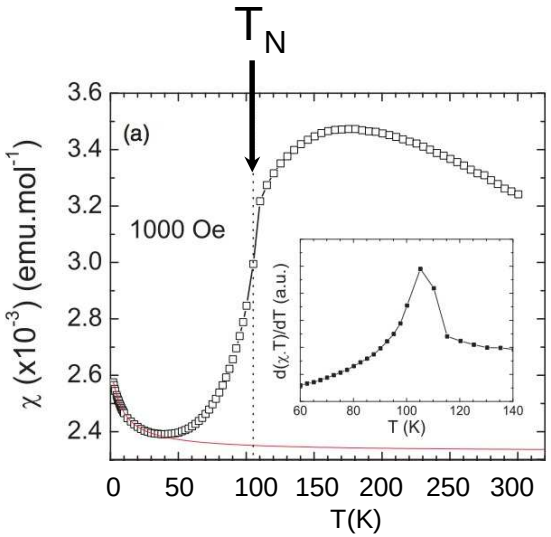

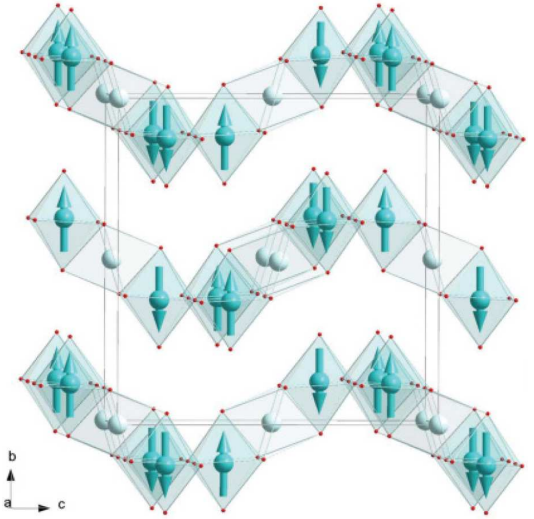

Y. Klein *et al.*
Phys. Rev. B **84** (2011) 054439

- Curie Constant consistent with three S=1 (low-spin) Ru^{4+} per trimer @ high temperature
- AFM ground-state of a new kind. From neutron diffraction :
  - Ru(2) show an AFM order
  - Ru(1) have NO ordered moments

Non-magnetic DOS

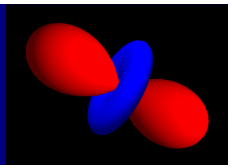

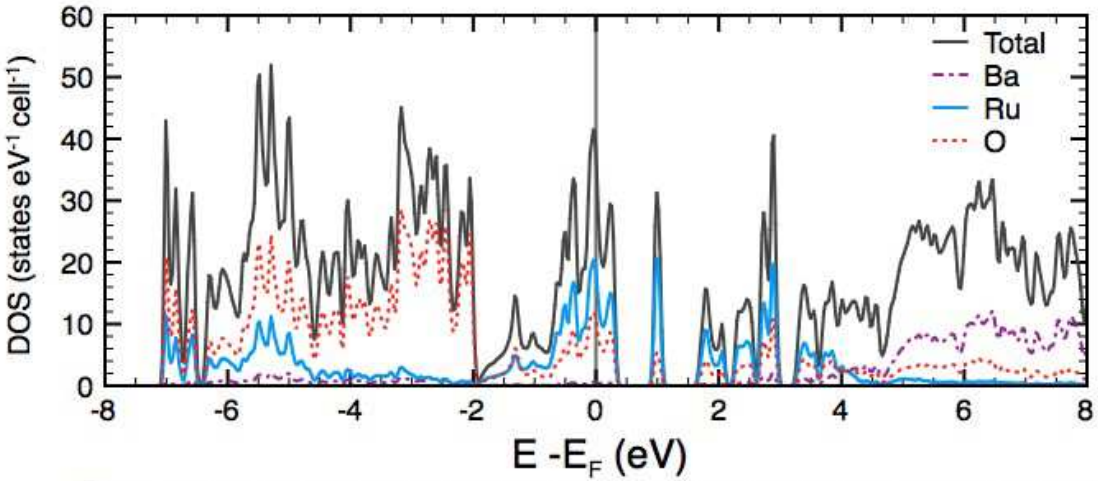

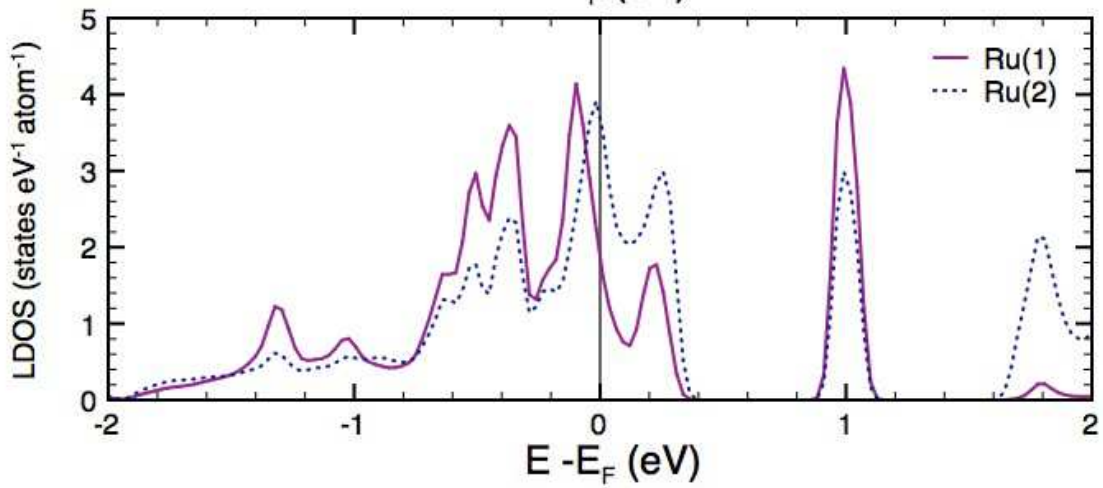

➡ Metallic
Filling of 2/3 of the Ru-t_{2g} orbitals :
$Ru(1)^{4+}$ and $Ru(2)^{4+}$

➡ $n(E_F)$ = 3.7 (eV atom)$^{-1}$ for Ru(2)
$n(E_F)$ = 1.8 (eV atom)$^{-1}$ for Ru(1)

➡ According to Stoner criterion, different behavior toward ferromagnetic instability

Non-magnetic DOS

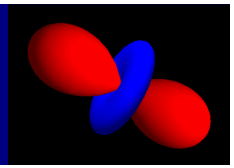

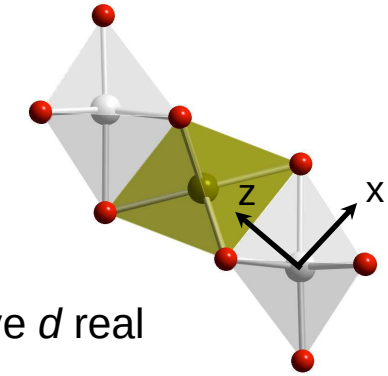

Alternative *d* real orbitals

$$|t_{2g}^{0}\rangle = |d_{z^2}\rangle$$

$$|t_{2g}^{+}\rangle = \sqrt{\frac{2}{3}}|d_{x^2-y^2}\rangle - \sqrt{\frac{1}{3}}|d_{xz}\rangle$$

$$|t_{2g}^{-}\rangle = \sqrt{\frac{2}{3}}|d_{xy}\rangle + \sqrt{\frac{1}{3}}|d_{yz}\rangle$$

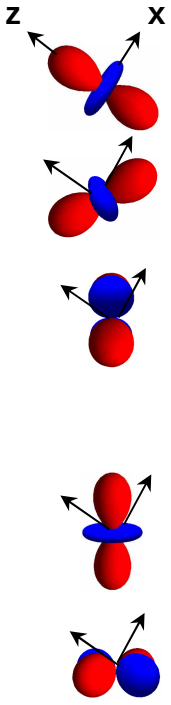

$$|e_{g}^{+}\rangle = \sqrt{\frac{1}{3}}|d_{x^2-y^2}\rangle + \sqrt{\frac{2}{3}}|d_{xz}\rangle$$

$$|e_{g}^{-}\rangle = \sqrt{\frac{1}{3}}|d_{xy}\rangle - \sqrt{\frac{2}{3}}|d_{yz}\rangle$$

We expect σ-bonding between $|t_{2g}^{0}\rangle$ states to form bonding, non-bonding and anti-bonding MOs:

$$|\psi_b\rangle = \frac{1}{\sqrt{4\left(1+\sqrt{2}S\right)}}\left(|\phi'_{(2)}\rangle + \sqrt{2}|\phi_{(1)}\rangle + |\phi''_{(2)}\rangle\right)$$

$$|\psi_{nb}\rangle = \frac{1}{\sqrt{2}}\left(|\phi'_{(2)}\rangle - |\phi''_{(2)}\rangle\right)$$

$$|\psi_{ab}\rangle = \frac{1}{\sqrt{4\left(1-\sqrt{2}S\right)}}\left(|\phi'_{(2)}\rangle - \sqrt{2}|\phi_{1}\rangle + |\phi''_{(2)}\rangle\right)$$

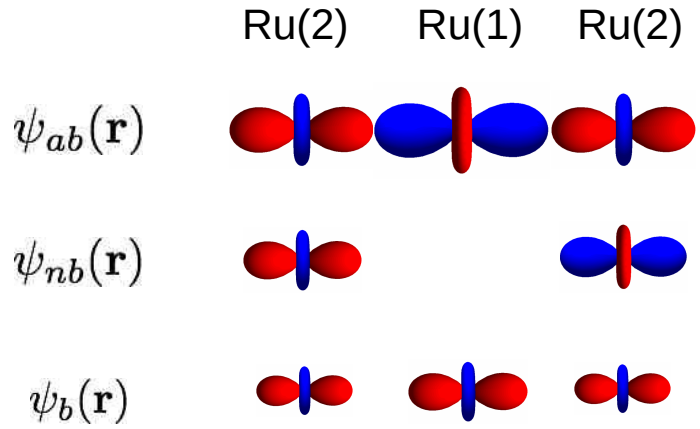

Non-magnetic DOS

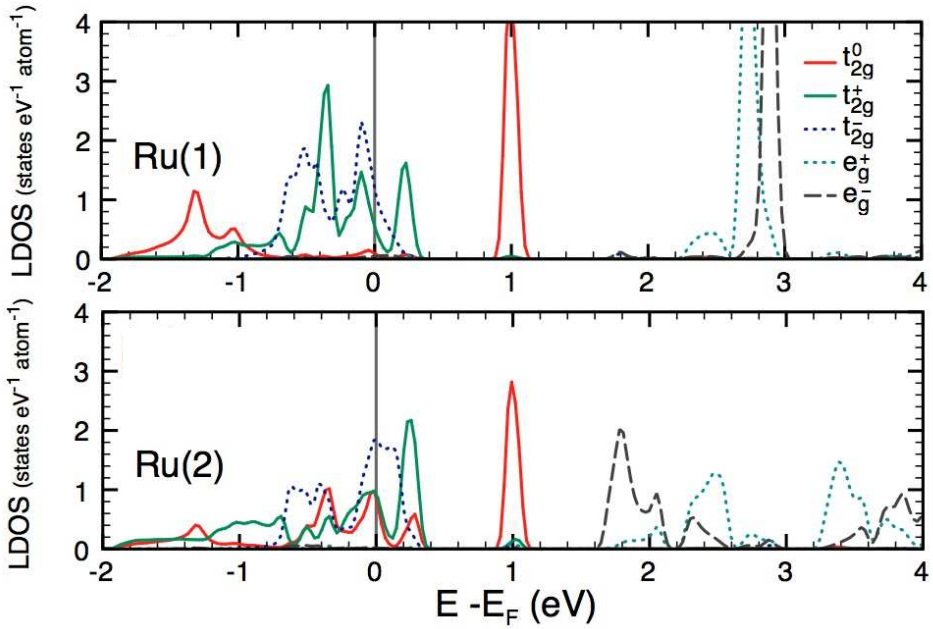

- $|t_{2g}{}^0\rangle$ are present at E_F for the Ru(2) but not for the Ru(1) : effect of metal-metal bonding
- The non-bonding MO has no Ru(1) component at E_F

Ferromagnetic calculations confirm the weaker polarization of Ru(1):

M (μ_B)	Ru(1)	Ru(2)
GGA	0.34	0.94
GGA+U	0.09	1.12

reduced from 2 μ_B expected for S=1 due to covalency

Definition of the couplings

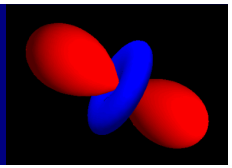

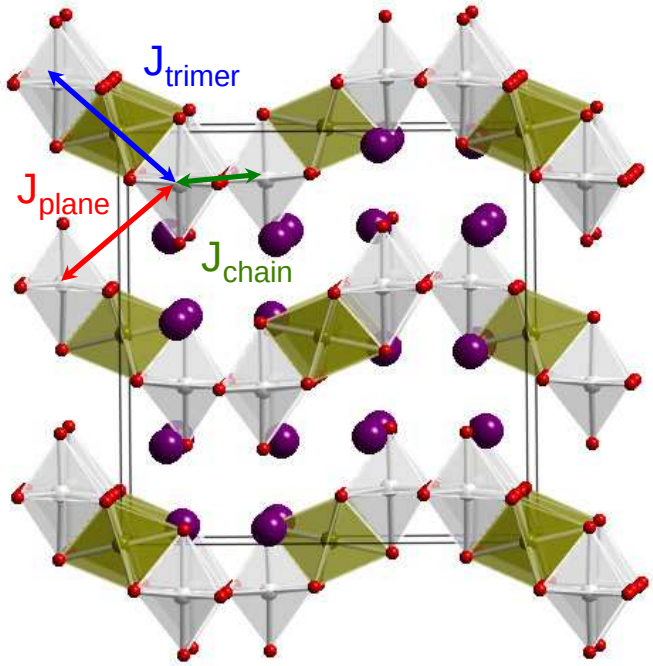

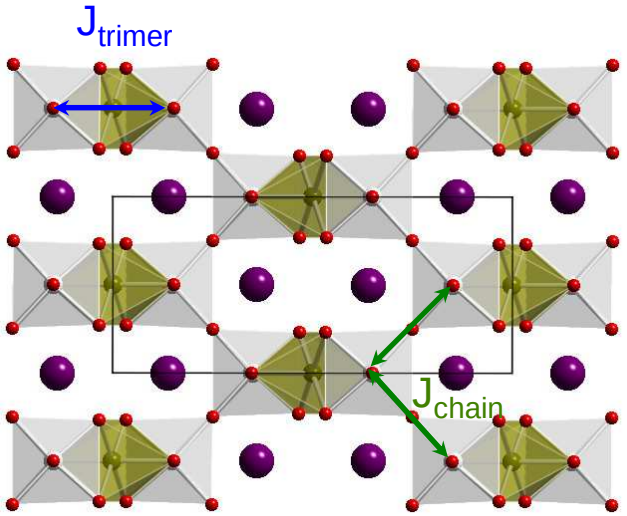

Mean value of the Heisenberg Hamiltonian on the DFT states (S=1 on Ru(2)) :

$$\epsilon_\alpha = \langle \alpha | \hat{H} | \alpha \rangle = \epsilon_0 + \sum_{i>j} J_{ij} \sigma_i \sigma_j \qquad \text{with} \qquad \sigma_i = \pm 1$$

Results : GGA and GGA+U

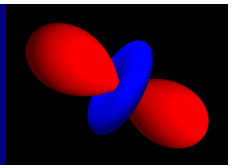

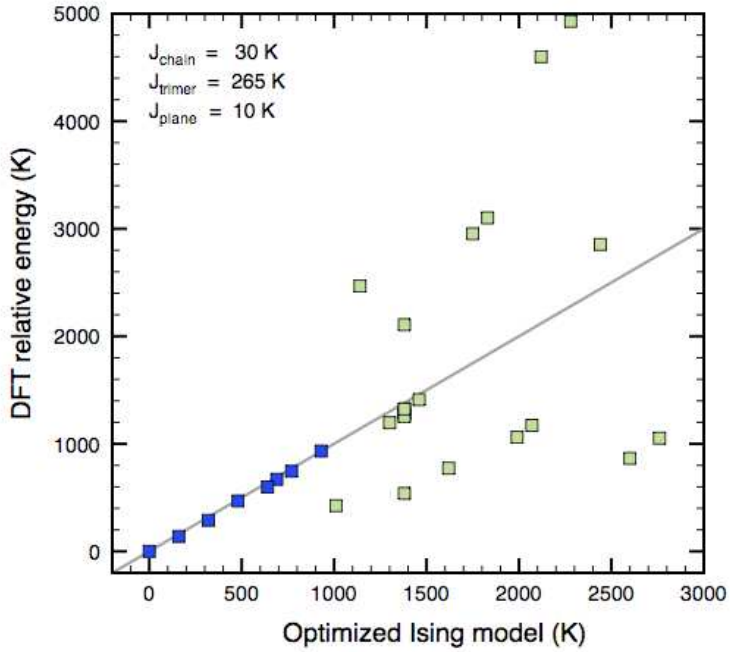

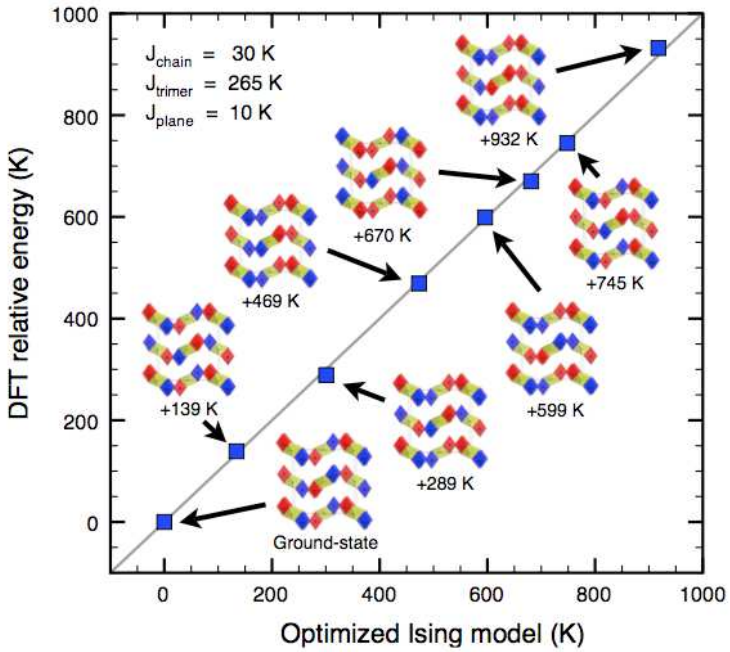

- No single set of J's can fit the entire spectrum of calculated magnetic excitations
- A subset of low energy configurations can be used instead

Ex. Int. (K)	J_{trimer}	J_{chain}	J_{plane}
GGA	344	86	25
GGA+U	265	30	10

Kinetic super-exchange mediated by Ru(1) :

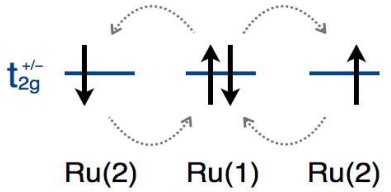

What about the susceptibility ?

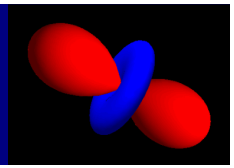

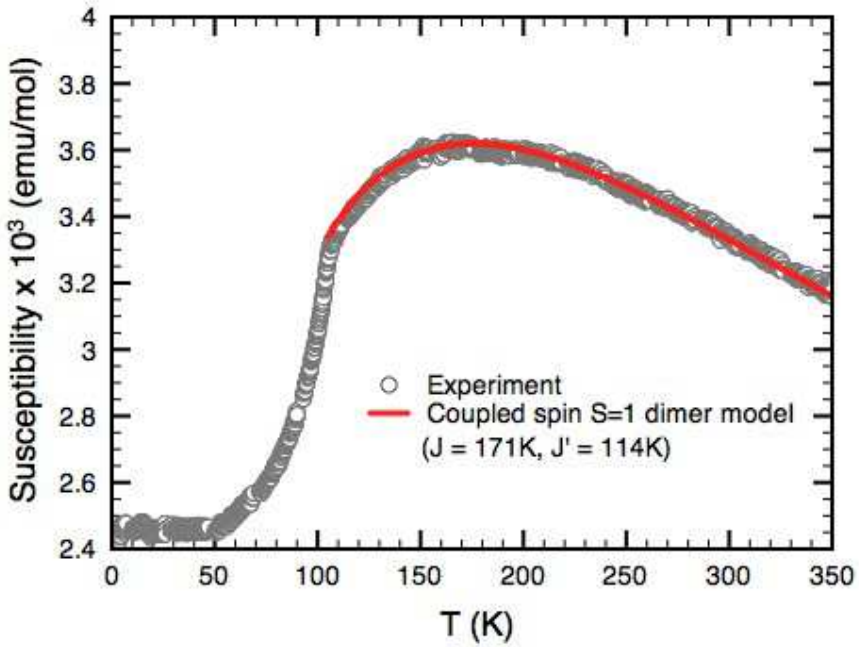

➡ Based on DFT results, the susceptibility is fit with a model of coupled (mean-field) spin S=1 dimers hold by Ru(2) :

$$\chi = \frac{\chi_{\mathrm{dim}}}{(1+\lambda\chi_{\mathrm{dim}})} + \chi_0$$

with :

$$\lambda = \frac{J_{\mathrm{inter}}}{N_A(g\mu_B)^2}$$

$$J_{\mathrm{inter}} \approx 2J_{\mathrm{chain}} + 2J_{\mathrm{plane}}$$

$$\chi_{\mathrm{dim}} = \frac{2\beta g^2\mu_B^2 N_A[1+5\exp(-2\beta J_{\mathrm{trimer}})]}{[3+\exp(\beta J_{\mathrm{trimer}})+5\exp(-2\beta J_{\mathrm{trimer}})]}$$

➡ Confirms the picture of strong AFM dimers coupled by weaker AFM inter-dimer interactions stabilizing a long-range Néel order.

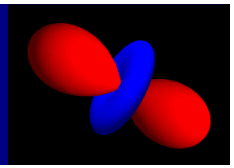

Thank you !

Breakdown of localized spin models ?

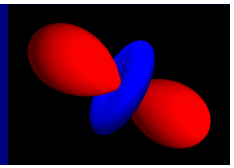

For a two-site, two-electron system :

The WF calculated in DFT for a FM spin arrangement

$$\psi^{\mathrm{KS}}(S_Z = 1) = \frac{1}{\sqrt{2}} \begin{vmatrix} \phi_a(\mathbf{r_1})\alpha(\sigma_1) & \phi_b(\mathbf{r_1})\alpha(\sigma_1) \\ \phi_a(\mathbf{r_2})\alpha(\sigma_2) & \phi_b(\mathbf{r_2})\alpha(\sigma_2) \end{vmatrix}$$

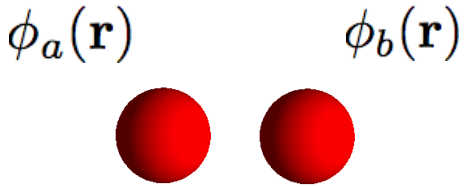

The WF calculated in DFT for a AFM spin arrangement

$$\psi^{\mathrm{KS}}(S_Z = 0) = \frac{1}{\sqrt{2}} \begin{vmatrix} \phi'_a(\mathbf{r_1})\alpha(\sigma_1) & \phi'_b(\mathbf{r_1})\beta(\sigma_1) \\ \phi'_a(\mathbf{r_2})\alpha(\sigma_2) & \phi'_b(\mathbf{r_2})\beta(\sigma_2) \end{vmatrix}$$

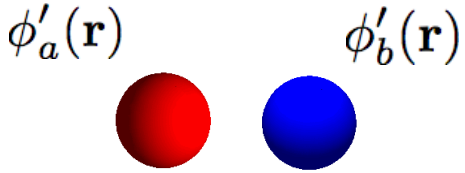

➡ The assumption that the spatial WF does not depend on the magnetic order is questionable for strongly covalent systems

Orbitals participating to the superexchange

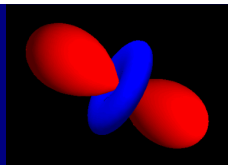

Electron density associated to a single V^{4+} ion : the only one in a flipped spin

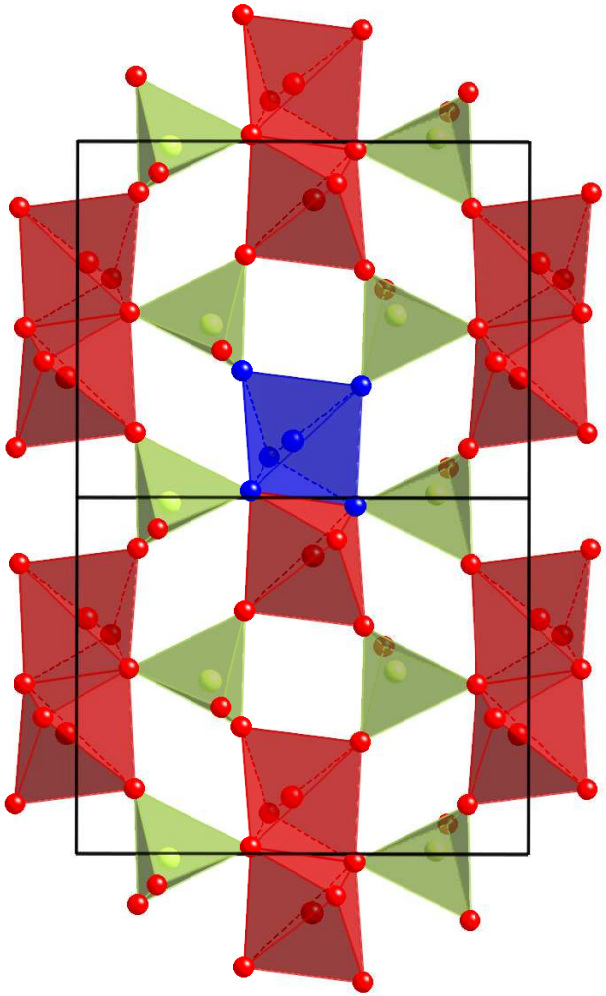

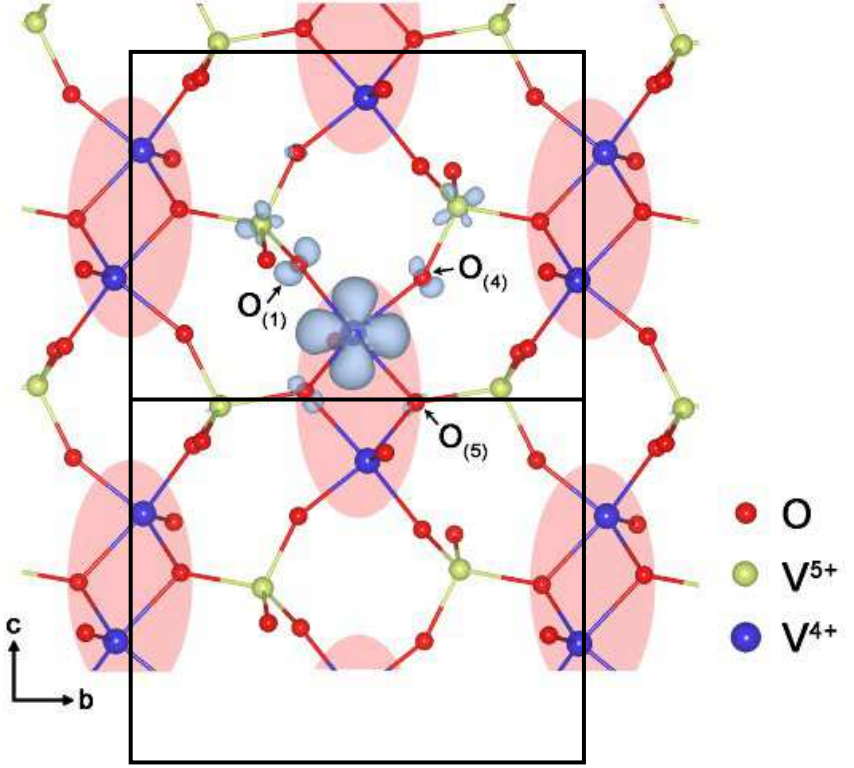

The magnetic orbital presents :

- Dominant $d_{y^2-z^2}$ orbital on the V^{4+} ion
- Specific p symmetry on the neighboring O
- Non zero density on the V^{5+} ion

The AFM ground-state

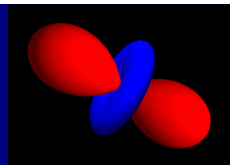

Both GGA and GGA+U predict the same AFM (exp.) ground-state order

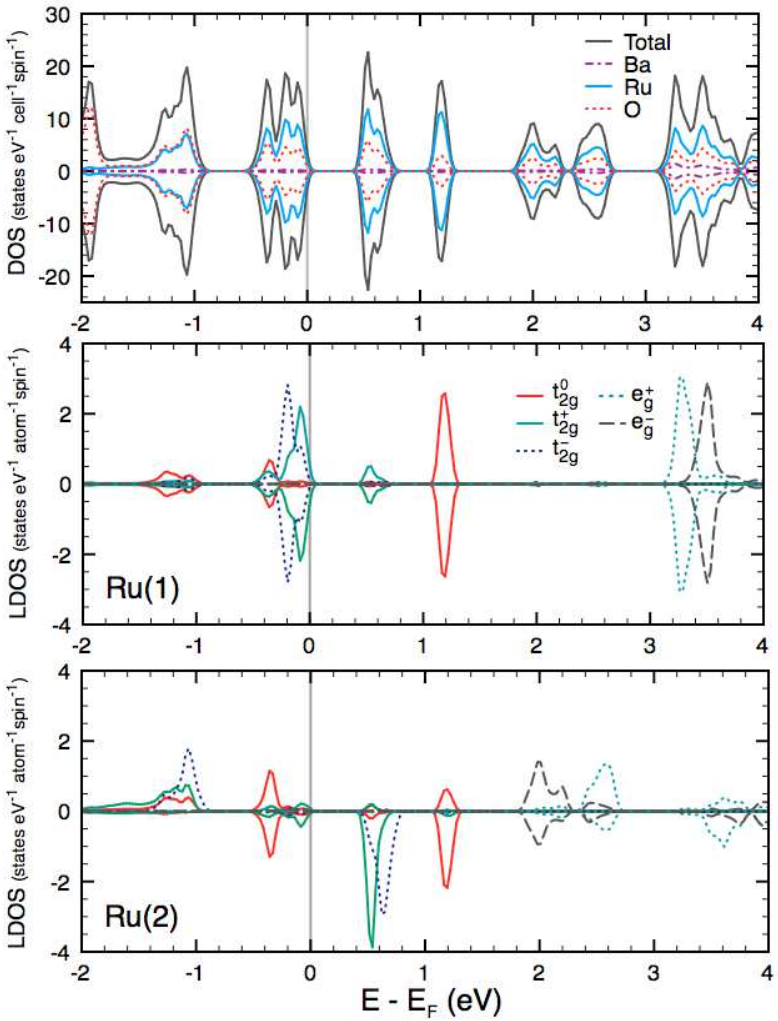

- Ru(2) hold a spin S=1 through the polarization of t_{2g}^{+} and t_{2g}^{-} states

  Ru(1) is paramagnetic through a double occupation of both t_{2g}^{+} and t_{2g}^{-} states

- Kinetic superexchange mechanism mediated by paramagnetic Ru(1) :